MSUCL-205
February 1976

A Study of the High-Spin Level Structure of ^{190}Pt and ^{192}Pt.*

J. C. Cunnane†, M. Piiparinen†† and P. J. Daly
Chemistry Department, Purdue University,
West Lafayette, Indiana 47907

and

C. L. Dors, T. L. Khoo and F. M. Bernthal
Departments of Chemistry and Physics and Cyclotron Laboratory,
Michigan State University, East Lansing, Michigan 48824

The level structures of the shape transitional nuclei ^{190}Pt and ^{192}Pt have been studied by $(\alpha,xn\gamma)$ reactions on enriched Os targets. The measurements included γ-ray singles, prompt and delayed γ-γ coincidences, half-life determinations in the range 1-500 ns, and γ-ray angular distributions. Detailed level schemes for ^{190}Pt and ^{192}Pt, incorporating much new spectroscopic information, are reported. Acute backbending observed at about spin 10 in the positive parity yrast sequences of the two nuclei is attributed to intersection of the ground bands by rotation aligned bands of both $(\nu i_{13/2}^{-2})$ and $(\pi h_{11/2}^{-2})$ character. A description of well-developed 5^- bands observed in both nuclei as semidecoupled $(\nu i_{13/2}, \nu j)$ bands is briefly discussed. 10^- isomers with half-lives of 47±6 ns in ^{190}Pt and 250±30 ns in ^{192}Pt are reported. The nature of these isomers is discussed in light of our related finding that the neighboring nuclei $^{189, 191, 193}$Pt have triaxial shapes ($\gamma \sim 30°$), and it is concluded that the 10^- states are predominantly of $(\nu i_{13/2}, \nu h_{9/2})$ two-quasiparticle composition.

NUCLEAR REACTIONS $^{190, 192}$Os$(\alpha,4n\gamma)$, $^{188, 190}$Os$(\alpha,2n\gamma)$, E = 28-50 MeV; measured E_γ, $I_\gamma(\theta)$, γ-γ coin, γ-t relationships; $^{190, 192}$Pt deduced level schemes, J, π, $T_{1/2}$.

I. INTRODUCTION

In an extensive series of experiments, the level structures of the nine Pt nuclei in the mass range A=186-194 have been studied by $(\alpha,xn\gamma)$ in-beam spectroscopy. These investigations were stimulated by the evidence for backbending behavior in the ground bands of even Os nuclei[1], by the discovery of the systematic occurrence of 5^-, 7^-, 9^-..... "bands" in Pt and Hg nuclei[2], and by Berkeley[3] and Jülich[4] results for odd and even mass Hg nuclei which can be satisfactorily understood in terms of rotation-alignment coupling[5]. The fact that the Pt nuclei span a region in which the prolate to oblate nuclear shape transition is believed to occur[6] has lent added interest to the present studies.

We have recently reported briefly on the dominant systematic features of the high-spin level spectra of the nine Pt nuclei[7]. Here the detailed results for the ^{190}Pt and ^{192}Pt nuclei are given. In discussing the implications of the findings, occasional reference will also be made to our results for the other Pt nuclei, which will be fully described in future publications. Concurrently with the present investigation, the ^{190}Pt and ^{192}Pt level structures have also been studied by Funke et al.[8]; generally, their results and ours are in excellent agreement.

II. EXPERIMENTAL PROCEDURES AND ANALYSIS

Targets approximately 10 mg/cm^2 thick of isotopically enriched ^{188}Os(87%), ^{190}Os(95%) and ^{192}Os(98%) imbedded in thin polystyrene films were prepared as described earlier[2]. These targets were bombarded with 1-5 nA beams of 30-50 MeV α-particles from the Michigan State University sector-focussed cyclotron and γ-ray data were acquired using several calibrated Ge(Li) spectrometers.

The γ-ray singles measurements were performed with a 10% Ge(Li) detector at 55° and a low energy photon Ge(Li) spectrometer (LEPS) at 125° to the beam direction. The resolution of the 10% spectrometer was 2.1 keV FWHM for 1332-keV γ-rays and that of the LEPS was 650 eV FWHM for 122-keV γ-rays. For all three Os targets, γ-ray spectra were recorded simultaneously with both spectrometers at α-particle bombarding energies of 30.9, 34.1, 37.0, 40.1, 42.8, 45.5 and 50.3 MeV. A typical γ-ray singles spectrum is illustrated in Fig. 1.

All the spectra were analyzed with the computer code SAMPO[9] and the intensity of each γ-ray was determined as a function of bombarding energy. In the present experiments, ^{192}Pt γ-rays were observed in the ^{192}Os(α,4n) and ^{190}Os(α,2n) reactions, and ^{190}Pt γ-rays in the ^{190}Os(α,4n) and ^{188}Os(α,2n) reactions. The isotopic assignments of individual γ-rays were initially based on the excitation function determinations, and were subsequently confirmed in γ-γ coincidence measurements, which were particularly valuable in assignments of the components of complex photopeaks.

Extensive γ-γ coincidence measurements were performed using two Ge(Li) detectors of ∿ 7% and ∿ 10% efficiency which were positioned on either side of the target at 180° to one another. Three parameter (γ,γ,t) coincidence data were accumulated and stored serially on magnetic tapes. Prompt coincidence events ($2\tau \sim 50$ ns) were later sorted using the MSU Sigma 7 computer, corrections for chance and Compton background coincidence events were applied, and coincidence spectra gated on each of 70-80 different γ-rays were obtained for each nucleus studied. Typical prompt coincidence spectra are shown in Figs. 2 and 3. Subsequently (see below), isomers with half-lives of 47 and 250 ns in ^{190}Pt and ^{192}Pt were discovered. Therefore, the coincidence data tapes for each nucleus were resorted with an appropriate time gate set on the delayed portion of the TAC spectrum and energy gates set on the strong γ-rays de-exciting the isomeric state. In this manner the γ-rays occurring in the cascades feeding the isomeric states were identified. In Fig. 4, the spectrum

of γ-rays populating the 250-ns isomer in ^{192}Pt is illustrated.

Short lifetime measurements were performed between cyclotron beam bursts using the LEPS spectrometer. Here, a prompt singles spectrum and nine delayed singles spectra spanning the time interval between beam-bursts (typically ∿ 50 ns) were accumulated. This technique was suitable for accurate determination of nuclear lifetimes in the range 1-30 ns. Longer lifetime measurements were performed in similar fashion using a beam-sweeping system which extended the interval between beam pulses incident on the target up to ∿ 500 ns. In these measurements the half-lives and the γ-rays de-exciting new 47±6 and 250±30 ns isomers in ^{190}Pt and ^{192}Pt, respectively, were determined. Representative prompt and delayed ^{192}Pt γ-ray spectra recorded using the beam-sweeping system are shown in Fig. 5.

For both the ^{190}Os(α,4n)^{190}Pt and ^{192}Os(α,4n)^{192}Pt reactions, angular distributions of the γ-radiations with respect to the beam direction were measured at five angles in the range 90°-140°. The γ-ray intensities at the different angles were normalized with respect to one another by assuming an isotropic distribution for the Os K x-rays. Typical experimental angular distributions for several γ-rays in ^{192}Pt are shown in Fig. 6. Values of the A_2/A_o and A_4/A_o coefficients were extracted from the data for all well resolved γ-rays of moderate to strong intensity in ^{190}Pt and ^{192}Pt. For weak or incompletely resolved γ-rays, the A_4/A_o coefficients were set equal to zero and values of A_2/A_o were extracted.

III. RESULTS

The construction of the level schemes was generally rather straightforward and was based primarily on the comprehensive γ-γ coincidence data, on the transition intensities and on energy sums. The excitation functions

determined for individual γ-rays were also useful, particularly in checking on the ordering of transitions within extensive cascades. Delayed γ-ray spectra recorded in the lifetime measurements provided clearcut information about the decay modes of isomeric states and were crucial in the determination of multipolarities, on the basis of intensity balance arguments, for a few important low-energy transitions. However, most of transition multipolarity and spin assignments were inferred from the γ-ray angular distribution data.

The ^{192}Pt level scheme

Table 1 lists the energies, relative intensities and angular distribution coefficients of the ^{192}Pt γ-rays observed in the ^{192}Os(α,4nγ)^{192}Pt reaction. Members of the ^{192}Pt ground band up to the 8^+ level at 2019 keV were previously known[2]. The main cascade of 662-, 544-, 375-, 105- and 501-keV stretched E2 transitions populating this 8^+ level, as shown in Fig. 7, was firmly established by the coincidence results, the transition intensities and the excitation functions. The energy of the $12^+ \rightarrow 10^+$ 105-keV transition was unexpectedly small, but the transition placement was solidly confirmed in short lifetime measurements, which yielded the result $t_{1/2}$ = 3.5±0.5 ns for the 12^+ level. The 662-, 544- and 375-keV γ-rays appeared only in the prompt γ-ray spectrum and a firm upper limit of 1.5 ns can be placed on the half-lives of the 14^+, 16^+ and 18^+ levels.

Convincing evidence was obtained for weaker γ-ray branches feeding into the positive parity yrast sequence at the 10^+ or 12^+ levels. Coincident 147- and 414-keV E2 transitions almost certainly occur in sequence between a second 14^+ level at 3080 keV and the 2519 keV 10^+ level; however, close examination of all the experimental data provided no clear indication as to the order of these equally intense transitions, and so they have not been included in Fig. 7.

The 3080-keV level appears to be fed by a 274-320 keV γ-ray cascade and, independently, by a 489-keV transition. The coincidence data also yielded evidence for a 279-427 keV γ-ray cascade which populates either the 2519-keV level or, less probably, the 12^+ level at 2624 keV.

The 5^-, 7^-, 9^- level sequence proposed earlier[2] was confirmed in the present study and the 11^- member of the sequence was also identified. A value of $t_{1/2}$ = 2.1±0.4 ns was determined for the 7^- level. The γ-γ coincidence and delayed γ-ray data, together with precise energy sums, firmly located the 250±30 ns isomeric state, de-exciting by 69- and 208-keV transitions, at 2172 keV. Analyses of the delayed γ-ray spectra (cf. Fig. 5) and intensity balance considerations settled several questions about transition multipolarities. For example, the observed intensity of the 581-keV ($6^+ \rightarrow 4^+$) γ-ray in these spectra showed that the 153-keV ($7^- \rightarrow 6^+$) transition must be E1 in character, thus removing any remaining doubt about the parity of the 5^-, 7^-, 9^-.... level sequence. More importantly, intensity balance requirements at the 2103- and 1965-keV levels showed that the 69-keV transition is predominantly M1 and the 208-keV transition predominantly E2 (regardless of the 446-keV transition multipolarity).

The question of the probable multipolarity of the 446-keV transition de-exciting the 1965-keV level posed a special problem. The angular distribution coefficients shown in Table 1 (as well as the values of A_2/A_o = 0.42±0.06 and A_4/A_o = -0.04±0.07 obtained when allowance was made for the isotropic contribution resulting from the partial feeding of the 1965-keV level through the 250-ns isomer) are not inconsistent with stretched E2 character. However, detailed examination of the (α,4n) excitation functions for the γ-rays de-exciting the 7^-, 9^- and 1965-keV levels and of the relative population cross sections for these levels observed in the (p,2nγ) and (α,2nγ) studies[2] led

us to the conclusion that the spin of the 1965-keV level must be less than 9, and is most probably 8. Subsequently, we learned of Rossendorf-Stockholm conversion coefficient measurements[8], which indeed showed that the 446-keV transition is predominantly M1. The angular distribution data are consistent with a $8^- \rightarrow 7^-$ assignment for the 446-keV transition, provided it is M1/E2 in character with a mixing ratio δ of about + 0.5. In ^{190}Pt (see below) and ^{194}Pt, analogous 8^- levels displaying very similar de-excitation characteristics have been identified in the present work.

The 2172-keV isomeric state is certainly of negative parity and its spin is most probably 10. By the delayed coincidence technique (cf. Fig. 4) the 188-, 228-, 237-, 320-, 339-, 253-, 396-, 411-, 439-, 454-, 510- and 673-keV γ-rays were identified as transitions preceding the isomer. The complex level structure above the 250-ns state was then constructed on the basis of the coincidence results and the transition intensities. It is noteworthy that the proposed (15^-) and (17^-) levels de-excite also to high-spin members of the positive parity yrast sequence and that these transition placements are firmly supported by the coincidence data.

Both the prompt and delayed coincidence results helped in the location of additional levels at 2584 and 2937 keV. Although analysis of the angular distributions did not lead to conclusive transition multipolarities assignments, the proposed I^π values of (10^+) and (12^+) seem most consistent with the available data.

Finally, we note that the members of the ^{192}Pt quasi γ-band observed in the (α,2nγ) studies[2] are not shown in Fig. 7, although these levels were found to be weakly populated in the (α,4n) reaction and a probable 7^+ member of the sequence at 2113 keV was identified. Similarly, the 6^- member of the 5^- band at 1746.5 keV is not included in Fig. 7; it too is populated much more strongly in the (α,2n) reaction. However, for completeness, the placements of the transitions de-exciting these levels are included in Table I.

The ^{190}Pt level scheme

The experimental results for the ^{190}Pt γ-rays observed in the ^{190}Os(α,4n) reaction are summarised in Table II. A similar approach to that described in the preceding section was used in constructing the ^{190}Pt level scheme shown in Fig. 8 on the basis of all the available data.

The main cascade of stretched E2 transition in ^{190}Pt extending up to the 16^+ level at 3577 keV was established by the γ-γ coincidence and excitation function results. Here again the $12^+ \rightarrow 10^+$ transition was found to be of unusually low energy (191 keV). The half-life of the 12^+ level was determined to be approximately 1.5 ns. In this nucleus, two additional moderately strong γ-rays, with energies of 787 and 688 keV, were found to populate the lowest 8^+ level directly. The angular distribution data indicated stretched E2 character for the 787-keV transition, thus establishing a 10^+ level at 2702 keV. On the other hand, the detailed coincidence results showed clearly that two γ-rays, of almost identical energy and of approximately equal intensity, contributed to the 688-keV photopeak observed in the singles spectra. It was not possible to determine multipolarities for the two 688-keV transitions from the measured angular distribution. However, a 123-688 keV γ-ray cascade connecting the 12^+ and 8^+ yrast levels was well established by the coincidence results and the only reasonable spin-parity assignment for the intermediate level at 2604 keV is 10^+. Thus, in ^{190}Pt there appears to be excellent evidence for the occurrence of three 10^+ levels within an energy interval of less than 170 keV.

A level at 3415 keV is established by the transitions populating the 12^+ and 14^+ yrast levels, and there is additional level structure, accommodating fairly intense transitions, built on the 3415-keV level (Fig. 8). The spins and parities of these high-lying levels are, however, uncertain.

The 5^-, 7^- and 9^- levels in ^{190}Pt were confirmed in the present work, and 11^- and (13^-) members of the sequence were identified. The half-life of the 7^- level was determined to be about 1.2 ns, but the experimental uncertainty is rather large because of the strong feeding of this level in the depopulation of the 47±6 ns isomeric state located at 2298-keV. γ-ray intensities determined in the beam-sweeping experiments were again valuable in establishing transition multipolarities from intensity balance requirements. The 47-ns isomer was found to de-excite by 75-keV M1 and 219-keV E2 transitions and it is quite clearly analogous to the 250-ns $(10)^-$ isomer in ^{192}Pt. It is interesting to contrast the observed angular distribution for the 219-keV γ-ray in ^{190}Pt, which is consistent with stretched E2 character, with the isotropic distribution observed for the corresponding 208-keV transition de-exciting the longer-lived ^{192}Pt $(10)^-$ isomer. All the experimental results showed that the 447-keV $8^- \rightarrow 7^-$ transition in ^{190}Pt is of very similar character to the ^{192}Pt 446-keV transition discussed in the preceding section. A 10^- level in ^{190}Pt at 2684 keV, which de-excites exclusively to the 8^- level, is also clearly established by the data.

The delayed coincidence spectra obtained by gating on the γ-rays de-exciting the 47 ns isomer identified the 142-, 251-, 273-, 303-, 454-, 524- and 541-keV γ-rays as transitions preceding the isomer. On the basis of the prompt coincidence results, an irregular sequence of levels, somewhat resembling the level structure built on the ^{192}Pt $(10)^-$ isomer, was constructed (Fig. 8). The weak 303-keV connection between the 3415-keV level and the $(13)^-$ level at 3112 keV is rather strongly indicated by both the prompt and delayed coincidence data.

The known[2] members of the ^{190}Pt quasi γ-band based at 598 keV and the 6^-

member of the 5^- band at 1834 keV are not shown in Fig. 8, but the transition placements are included in Table II. In earlier work[10], isomers with half-lives of 145 and 95 μs were ascribed to ^{190}Pt and ^{192}Pt, respectively, but in the course of the present studies, we have determined that these isomers should be re-assigned to ^{189}Pt and ^{191}Pt, respectively[11].

IV. DISCUSSION

The ^{190}Pt and ^{192}Pt level spectra resemble one another closely and exhibit a variety of interesting high-spin structural features. In each nucleus, the 4^+ ground band member is populated by two γ-ray cascades of roughly equal intensity, one involving even-spin positive parity levels and the other a family of negative parity levels starting with 5^-. An additional obvious similarity is the occurrence of a 10^- isomer at about 2.2 MeV excitation energy in each nucleus. These isomeric states and the level structures built upon them play a prominent part in the nuclear de-excitation.

In both ^{190}Pt and ^{192}Pt, the low-lying positive parity levels up to 8^+ form ground state bands typical of soft, weakly deformed rotors, and the level energies can be satisfactorily reproduced using a variable moment-of-inertia treatment (VMI). However, above the 8^+ levels, the level energies depart drastically from VMI predictions, and the observed separations of the lowest 10^+ and 12^+ levels are remarkably small. The overall positive parity yrast sequences of these nuclei display a type of backbending behavior which is much more acute than the intensively studied backbending observed in many rare earth prolate nuclei. In Refs. 7 and 8, this striking structural phenomenon has been discussed in some detail, with the common conclusion that rotation-aligned bands of $(\nu i_{13/2}^{-2})$ and/or $(\pi h_{11/2}^{-2})$ character must intersect the ground bands of ^{190}Pt and ^{192}Pt at excitation energies of about 2.5 MeV. Our proposal is that the two-proton and two-neutron rotation-aligned structures are <u>both</u> important in interpreting the observed spectra, particularly in accounting for the three close-lying 10^+ states in ^{190}Pt and for the two close-lying 10^+ states in ^{192}Pt. In ^{190}Pt, we have interpreted the 2604 keV level as the 10^+ ground band member and have suggested dominant intrinsic configurations of $(\pi h_{11/2}^{-2})$ for the 2536-keV level, and $(\nu i_{13/2}^{-2})$ for the 2702-keV 10^+ and 2727-keV 12^+ levels. In ^{192}Pt, likely dominant configurations are $(\pi h_{11/2}^{-2})$ for the

2519-keV level and $(\nu i_{13/2}^{-2})$ for the 2583- and 2623-keV levels. (A VMI extrapolation of the ^{192}Pt ground band suggests that its 10^+ member lies above 2.7 MeV). These assignments were found to be consistent with the measured $12^+ \rightarrow 10^+$ B(E2) values and with the branching intensities in the decay of the ^{190}Pt 2727-keV level, when the expected mixing between the 10^+ and 12^+ members of the ground bands and of the $(\pi h_{11/2}^{-2})$ and $(\nu i_{13/2}^{-2})$ rotation aligned bands was taken into account. This was demonstrated by performing a simple three-band mixing calculation, assuming that the $12^+ \rightarrow 10^+$ B(E2) matrix element within each particular configuration has the full collective strength of a ground band transition. (While admixtures of several different Nilsson orbitals contribute to the composition of the "yrast states" of, for example, the $\nu i_{13/2}$ two-quasiparticle family, they all contribute with the same phase; consequently, the E2 matrix elements connecting such states are coherent.) For the matrix elements $\langle g.b.|H|\nu i_{13/2}^{-2}\rangle$, $\langle g.b.|H|\pi h_{11/2}^{-2}\rangle$ and $\langle \pi h_{11/2}^{-2}|H|\nu i_{13/2}^{-2}\rangle$, two choices[12] which gave good agreement with the data are -30, -30, 0 and -20, -20, -20 keV.

The specific assignments proposed for the various 10^+ and 12^+ levels are not yet firmly established, and indeed they differ in some instances from those favored by the Rossendorf-Stockholm team[8]. It does not seem possible to resolve the points of disagreement in any decisive way with the data currently available; in this regard, measurements of lifetimes and g-factors for some of the 10^+ and 12^+ levels would be most helpful. However, we do argue strongly that both the $(\nu i_{13/2}^{-2})$ and $(\pi h_{11/2}^{-2})$ rotation-aligned states must play major roles in determining the positive parity level structure in these nuclei. Some involvement of the $(\pi h_{11/2}^{-1}, \pi h_{9/2})$ $J^\pi = 10^+$ configuration is also a possibility.

Bands of 5^-, 7^-, 9^- ----- levels are now known in many even-even Hg and

Pt nuclei[2-4] and even-spin bandmembers have also been located in some of the Hg nuclei[13]. In the present study, several new members of the 5^- bands in ^{190}Pt and ^{192}Pt have been identified, and the $7^- \rightarrow 5^-$ E2 transitions have been found to be enhanced to about the same extent as the $2^+ \rightarrow 0^+$ ground band transitions. The proposal that these negative parity sequences constitute rotation-aligned bands with microscopic composition dominated by two-neutron components of the type $(\nu i_{13/2}, \nu j)$ has recently been tested in model calculations by Neergård et al.[14]. These calculations were generally successful in reproducing the observed energies and de-excitation properties of the negative parity states in the Hg nuclei, but were less successful for the Pt nuclei, where the 5^- and 7^- states occur 300-400 keV lower than in the Hg nuclei. In Ref. 14, it was suggested that a more realistic treatment of the effective interaction (such as RPA) might improve the agreement with the experimental findings in the Pt nuclei. In any case, there seems little doubt that the Pt 5^- bands are of the same nature as the Hg 5^- bands. In the odd-A Pt nuclei, $21/2^-$ bands arising from combinations of the $\nu i_{13/2}^{-1}$ state with members of the 5^- bands seen in the neighboring core nuclei have been systematically observed[7]. As has been pointed out in connection with analogous $21/2^-$ bands in odd-A Hg nuclei, the spin of 21/2 occurs because the second $i_{13/2}$ neutron can be aligned to a maximum spin of 11/2 only[3,4]. A final noteworthy point is that the 8^- states in ^{190}Pt and ^{192}Pt are observed to de-excite exclusively to the 7^- bandmembers, just as is predicted by the calculations[14] for the 8^- states in the Hg nuclei. It is a consequence of this branching that the 6^- bandmembers are only weakly populated in the $(\alpha,4n)$ reactions, whereas they were found to be quite strongly populated in earlier $(\alpha,2n\gamma)$ measurements[2].

It is interesting to consider the nature of the 10^- isomeric states in ^{190}Pt and ^{192}Pt. In the de-excitation of these isomers, the reduced transi-

tion probabilities derived from the data are B(M1,75 keV) = 1.8×10^{-4} s.p.u. and B(E2,219 keV) = 1.2×10^{-1} s.p.u. in ^{190}Pt, and B(M1,69 keV) = 4.8×10^{-5} s.p.u. and B(E2,208 keV) = 1.7×10^{-2} s.p.u. in ^{192}Pt. The rather large hindrance factors indicate clearly that the 10^- isomers are structurally quite different from the members of the 5^- bands. No two-quasiparticle 10^- combination seems possible using the proton orbitals available in this region. Instead, these 10^- isomers must be of two-neutron character and they are very probably closely related to the known[15] 11/2[615]ν, 9/2[505]ν 10^- isomer at 1706 keV in ^{190}Os. One complicating factor is that our recent studies[16] of rather complete $\nu i_{13/2}$ level families in ^{189}Pt, ^{191}Pt and ^{193}Pt indicate strongly that these nuclei have triaxial shapes with asymmetry parameters γ close to 30°. Consequently, the question arises whether a description of the ^{190}Pt, ^{192}Pt 10^- isomers in terms of Nilsson designations appropriate to axially symmetric prolate nuclei (i.e. γ = 0°) implies that these are shape isomers.

In a companion paper[11], evidence for the existence of two low-lying isomers in each of the isotopes ^{189}Pt and ^{191}Pt is presented. In each case, the upper isomer is the $13/2^+$ member of the $\nu i_{13/2}$ family and it de-excites to a lower-lying $9/2^-$ isomer, which is derived from the $\nu h_{9/2}$ shell model state. Accordingly, the occurrence of $(\nu i_{13/2}, \nu h_{9/2})$ isomeric states can reasonably be expected in neighboring even-A Pt isotopes at energies somewhat lower than two-quasiparticle excitations arising from a broken $\nu i_{13/2}$ pair. A straightforward application of level systematics would suggest $J^\pi = 11^-$ for the ^{190}Pt, ^{192}Pt isomers rather than the observed 10^- values. However, in ^{193}Pt, ^{191}Pt and ^{189}Pt, the $11/2^+$ members of the $\nu i_{13/2}$ families have been located just above the $13/2^+$ isomers. The $11/2^+$ to $13/2^+$ energy spacing is found to decrease as A decreases (and as γ decreases) until the two levels are almost degenerate in ^{189}Pt, a trend which is in excellent agreement with

triaxial rotor calculations[16]. For values of γ less than about 25°, the $11/2^+$ level is predicted to drop below the $13/2^+$ level. The observation of 10^- rather than 11^- isomers in ^{190}Pt, ^{192}Pt therefore seems to indicate that the $(\nu i_{13/2}, \nu h_{9/2})$ configuration favors smaller γ-values than those derived from the $\nu i_{13/2}$ families in the neighboring odd-A nuclei. We do not have a satisfactory physical understanding of this result. We note, however, that in Larsson's theoretical investigation[17] of the dependence of single particle energies on γ in the Os-Pt region, the orbital designated 9/2[505] in the prolate limit was shown to slope steeply downwards in energy as γ decreases from 30° to 0°. Occupation of this orbital by a particle would thus be expected to favor smaller values of γ. In summary, the present data and energy level systematics favor the interpretation of the ^{190}Pt and ^{192}Pt isomers as two-quasiparticle states of $(\nu i_{13/2}, \nu h_{9/2})$ character, but some interesting questions about the detailed nature of these states remain unanswered. Here again, g-factor determinations might prove to be illuminating.

We thank S. K. Saha for helping with some of the measurements and G. F. Bertsch and F. S. Stephens for stimulating discussions.

References

*Research supported by the U.S. Energy and Development Administration and the National Science Foundation.

†Present address: Schuster Laboratory, University of Manchester, England.

††Present address: Physics Dept., University of Jyväskylä, Finland.

1. R. A. Warner, F. M. Bernthal, J. S. Boyno and T. L. Khoo, Phys. Rev. Lett. 31, 835 (1973).
2. S. W. Yates, J. C. Cunnane, R. Hochel and P. J. Daly, Nucl. Phys. A222, 301 (1974).
3. D. Proetel, D. Benson, Jr., A. Gizon, J. Gizon, M. R. Maier, R. M. Diamond and F. S. Stephens, Nucl. Phys. A226, 237 (1974); D. Proetel, R. M. Diamond and F. S. Stephens, ibid. A231, 301 (1974).
4. H. Beuscher, W. F. Davidson, R. M. Lieder, A. Neskakis and C. Mayer-Boricke, Phys. Rev. Lett. 32, 843 (1974).
5. F. S. Stephens, R. M. Diamond and S. G. Nilsson, Phys. Lett. 44B, 429 (1973).
6. S. Frauendorf and V. V. Pashkevich, Phys. Lett. 55B, 365 (1975).
7. M. Piiparinen, J. C. Cunnane, P. J. Daly, C. L. Dors, F. M. Bernthal and T. L. Khoo, Phys. Rev. Lett. 34, 1110 (1975).
8. L. Funke, P. Kemnitz, G. Winter, S. A. Hjorth, A. Johnson and Th. Lindblad, Phys. Lett. 55B, 436 (1975) and preprint.
9. J. T. Routti and S. G. Prussin, Nucl. Instrum. Methods 72, 125 (1969).
10. I. A. Fraser and R. B. Moore, Bull. Am. Phys. Soc. 12, 715 (1967).
11. M. Piiparinen et al., Phys. Rev. (the following paper).
12. Using a two-body interaction derived from Brueckner theory, the matrix element, $\langle \nu i_{13/2}^{-2} | H | \pi h_{11/2}^{-2} \rangle_{J=10}$, is estimated to be ∿ 10 keV (G. F. Bertsch, private communication)

13. R. M. Lieder, H. Beuscher, W. F. Davidson, A. Neskakis and C. Mayer-Boricke, Nucl. Phys. A248, 317 (1975).
14. K. Neergård, P. Vogel and M. Radomski, Nucl. Phys. A238, 199 (1975).
15. A. W. Sunyar, G. Scharff-Goldhaber and M. Mc Keown, Phys. Rev. Lett. 21, 237 (1968).
16. T. L. Khoo, F. M. Bernthal, C. L. Dors, M. Piiparinen, S. K. Saha, P. J. Daly and J. Meyer-ter-Vehn, Phys. Lett. (in press).
17. S. E. Larsson, Physica Scripta 8, 17 (1973).

TABLE I. Transitions in ^{192}Pt from $^{192}Os(\alpha,4n)$ reaction observed with 45.5 MeV incident α-particles.

γ-ray energy[a] (keV)	Relative intensity[a] at 125°	Angular Distribution A_2/A_o	Angular Distribution A_4/A_o	Inferred Multipolarity	Placement (keV)
69.12(10)	37(3)			M1	2172→2103
104.73(10)	48(4)	0.27±0.05	-0.18±0.06	E2	2624→2519
134.46(10)	206(12)	0.14±0.03	-0.09±0.03	E2	1518→1384
147.07(12)	30(3)	0.28±0.05	-0.18±0.07	E2	see text
152.98(12)	34(3)	-0.11±0.05	-0.01±0.06	E1	1518→1365
160.10(20)	10(1)				4321→4161
183.04(20)	17(2)				1384→1201
188.03(20)	22(2)				3883→3695
207.93(15)	46(4)	0.06±0.06		E2	2172→1965
210.3(5)	8(2)				2313→2103
228.34(15)	33(3)	0.31±0.05	-0.19±0.06	E2	3924→3695
236.84(16)	23(2)				4161→3924
273.83(18)	19(2)	-0.55±0.09		(M1/E2)	see text
279.57(18)	19(2)				see text
295.96(12)	66(5)	-0.02±0.04			612→316
308.44(12)	34(3)	0.04±0.05			921→612
316.50(5)	1000	0.19±0.03	-0.10±0.03	E2	316→0
319.9(4)	∿25				see text
339.37(20)	75(8)	-1.21±0.19		(E2/M1)	2512→2103
353.00(12)	38(3)	0.34±0.07	-0.11±0.09	E2	2937→2584
362.54(15)	24(2)				1747→1387
374.51(12)	128(10)	0.28±0.04	-0.16±0.05	E2	2998→2624

Table 1. (contd)

γ-ray energy (keV)	Relative intensity at 125°	Angular Distribution A_2/A_o	Angular Distribution A_4/A_o	Inferred Multipolarity	Placement (keV)
381.5(3)	8(3)				3924→3542
395.64(20)	21(3)	<0		(M1)	3022→2627
398.73(23)	20(3)				
411.03(20)	27(3)	0.44±0.08			2584→2172
414.04(16)	54(5)	0.42±0.07		(E2)	see text
416.8(5)	11(4)				1201→785
426.91(18)	40(4)	0.44±0.07		(E2)	see text
438.5(3)	7(2)				2950→2512
446.10(10)	141(11)	0.27±0.03	-0.01±0.05	(M1/E2)	1965→1518
454.32(25)	79(8)	0.34±0.05		(E2)	2627→2172
468.06(5)	955(57)	0.18±0.02	-0.11±0.03	E2	785→316
470.93(20)	21(4)				
485.3(3)	10(2)				1406→921
489.2(3)	∿40	-0.85±0.15		(M1/E2)	see text
500.62(10)	329(23)	0.27±0.03	-0.13±0.04	E2	2519→2019
510.4(5)	78(20)				3022→2512
531.5(3)	12(2)				
543.85(20)	45(4)	0.43±0.07		(E2)	3542→2998
548.8(3)	11(2)				
552.1(3)	22(3)				2517→1965
561.0(3)	20(3)				1482→921
564.9(4)	37(11)				2584→2019
565.8(5)	28(9)	0.37±0.06			2530→1965
580.88(12)	450(32)	0.24±0.03	-0.15±0.04	E2	1365→785
584.89(12)	267(19)	0.13±0.03	-0.09±0.04	E2	2103→1518

Table 1 (contd)

γ-ray energy (keV)	Relative intensity at 125°	Angular Distribution A_2/A_o	Angular Distribution A_4/A_o	Inferred Multipolarity	Placement (keV)
588.67(20)	28(3)				1201→612
599.40(12)	498(35)	-0.16±0.03	-0.07±0.07	E1	1384→785
605.92(25)	33(4)	0.38±0.08		(E2)	2709→2103
612.6(3)	9(2)				612→0
615.8(3)	14(3)				
631.5(4)	12(3)				2113→1482
648.4(5)	15(3)				
653.05(16)	386(31)	0.24±0.03	-0.15±0.03	E2	2019→1365
662.1(3)	20(3)	0.32±0.10		(E2)	4204→3542
673.01(25)	70(7)	0.21±0.04	-0.14±0.05	E2	3695→3022
697.0(3)	40(5)	-0.18±0.06		(E1)	3695→2998
746.5(4)	12(3)				

[a]Uncertainties in the least significant figures are indicated in parentheses.

TABLE II. Transitions in ^{190}Pt from ^{190}Os(α,4n) reaction observed with 45.5 MeV incident α-particles

γ-ray[a] energy (keV)	Relative[a] intensity at 125°	Angular distribution A_2/A_o	Angular distribution A_4/A_o	Inferred Multipolarity	Placement (keV)
75.0(5)	20(6)			M1	2298→2223
123.2(3)	7(2)				2727→2604
141.8(2)	14(3)				3808→3666
166.6(1)	216(22)	0.28±0.10	-0.13±0.10	E2	1631→1465
191.4(1)	119(10)	0.31±0.10	-0.19±0.10	E2	2727→2535
217.2(3)	15(2)	-0.83±0.30		(M1/E2)	
219.1(2)	47(5)	0.32±0.10		(E2)	2298→2079
227.3(3)	12(2)				
251.2(2)	59(5)	0.36±0.18	-0.16±0.15	E2	3666→3415
273.3(2)	49(4)	-0.72±0.12		(M1/E2)	2571→2298
295.7(1)	1000	0.24±0.11	-0.10±0.09	E2	296→0
301.8(1)	74(6)				598→296
303.3(5)	15(5)				3415→3112
306.6(3)	23(3)				
319.0(3)	27(3)	0.44±0.16		(M1/E2)	917→598
336.4(2)	49(5)	-0.19±0.09		(E1)	1465→1128
342.6(3)	114(11)	0.51±0.18		(E2)	3069→2727
343.5(3)	142(12)	-0.10±0.08		E1	1631→1288
345.7(3)	27(3)	0.42±0.16			3415→3069
369.4(4)	17(2)				1834→1465
376.5(4)	21(2)	0.49±0.18			
391.8(4)	20(2)				1128→737

Table II (contd)

γ-ray energy[a] (keV)	Relative intensity[a] at 125°	Angular distribution A_2/A_o	Angular distribution A_4/A_o	Inferred Multipolarity	Placement (keV)
412.6(4)	16(2)				
417.1(3)	32(3)				4083 3666
420.0(4)	17(2)				
441.2(1)	931(56)	0.30±0.12	-0.08±0.10	E2	737→236
447.4(2)	138(11)	0.58±0.24	0.04±0.24	(M1/E2)	2079→1631
453.9(5)	18(4)	-1.32±0.35		(M1/E2)	3025→2571
507.2(4)	38(7)				3577→3069
524.3(3)	34(4)	0.34±0.12		(E2)	2822→2298
530.7(3)	61(6)	0.39±0.10			1128→598
533.1(3)	28(3)				1450→917
538.3(3)	56(6)	0.23±0.10		(E2)	2761→2223
541.0(3)	42(5)	0.35±0.12		(E2)	3112→2571
550.7(2)	566(40)	0.37±0.11	-0.10±0.09	E2	1288→737
538.7(3)	49(5)				3345→2716
591.5(2)	199(18)	0.26±0.12	-0.16±0.10	E2	2223→1631
597.6(4)	39(4)				598→0
605.1(4)	41(5)				2684→2079
612.8(5)	15(3)				
620.0(2)	255(23)	0.35±0.09	-0.14±0.07	E2	2535→1915
627.7(2)	377(34)	0.39±0.08	-0.10±0.06	E2	1915→1288
637.8(5)	12(3)				
654.4(4)	17(3)				
688.1(6)[b]	103(11)				2604→1915 3415→2727
727.6(2)	291(30)	0.25±0.12	-0.06±0.10	E1	1465→737
786.5(3)	51(6)	0.27±0.20	-0.09±0.19	E2	2702→1915

Table II (Contd)

[a]Uncertainties in the least significant figures are indicated in parentheses.

[b]Doublet.

Figure Captions

Fig. 1. A γ-ray singles spectrum measured with the LEPS spectrometer for 45.5-MeV α-particles incident on the ^{190}Os target.

Fig. 2. Some important γ-γ coincidence spectra obtained in the ^{192}Pt study.

Fig. 3. Some important γ-γ coincidence spectra obtained in the ^{190}Pt study.

Fig. 4. A spectrum of γ-rays in delayed coincidence with the strong γ-rays de-exciting the 10^- isomer in ^{192}Pt.

Fig. 5. The prompt (upper) and most delayed (lower) ^{192}Pt γ-ray spectra recorded using the beam-sweeping system, and (inset) the decay data used to determine the 10^- isomeric half-life.

Fig. 6. Samples of the γ-ray angular distribution data for ^{192}Pt.

Fig. 7. The ^{192}Pt level scheme. The widths of the transition arrows are proportional to the transition intensities.

Fig. 8. The ^{190}Pt level scheme. The widths of the transition arrows are proportional to the transition intensities.

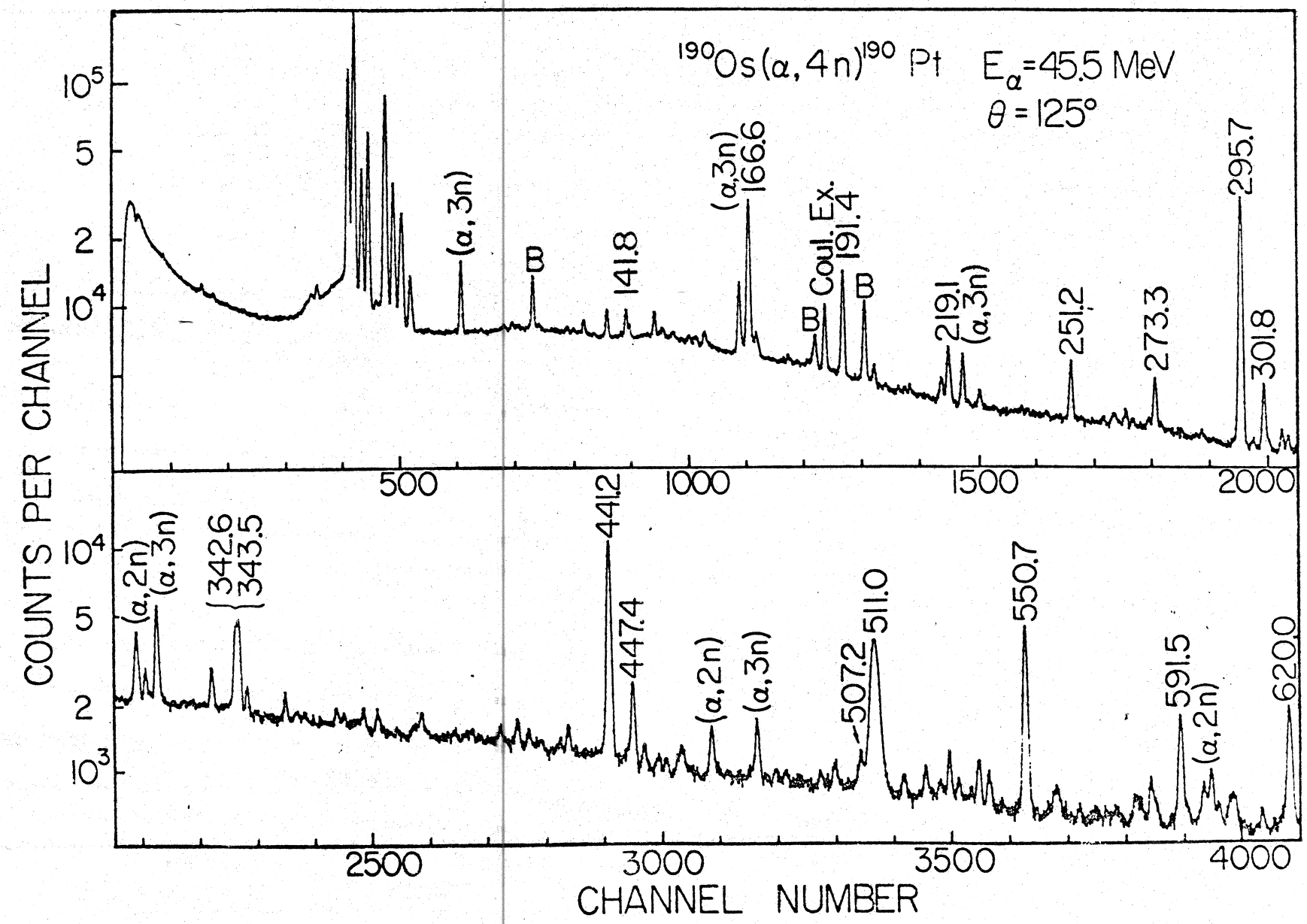
^{190}Os(α, 4n)^{190} Pt
E_α=45.5 MeV
θ = 125°
(α, 3n)
141.8
(α,3n)
166.6
Coul. Ex.
191.4
219.1
(α,3n)
251.2
273.3
295.7
301.8
(α,2n)
(α,3n)
342.6
343.5
441.2
447.4
(α,2n)
(α,3n)
507.2
511.0
550.7
591.5
(α,2n)
620.0
COUNTS PER CHANNEL
CHANNEL NUMBER

Fig. 1

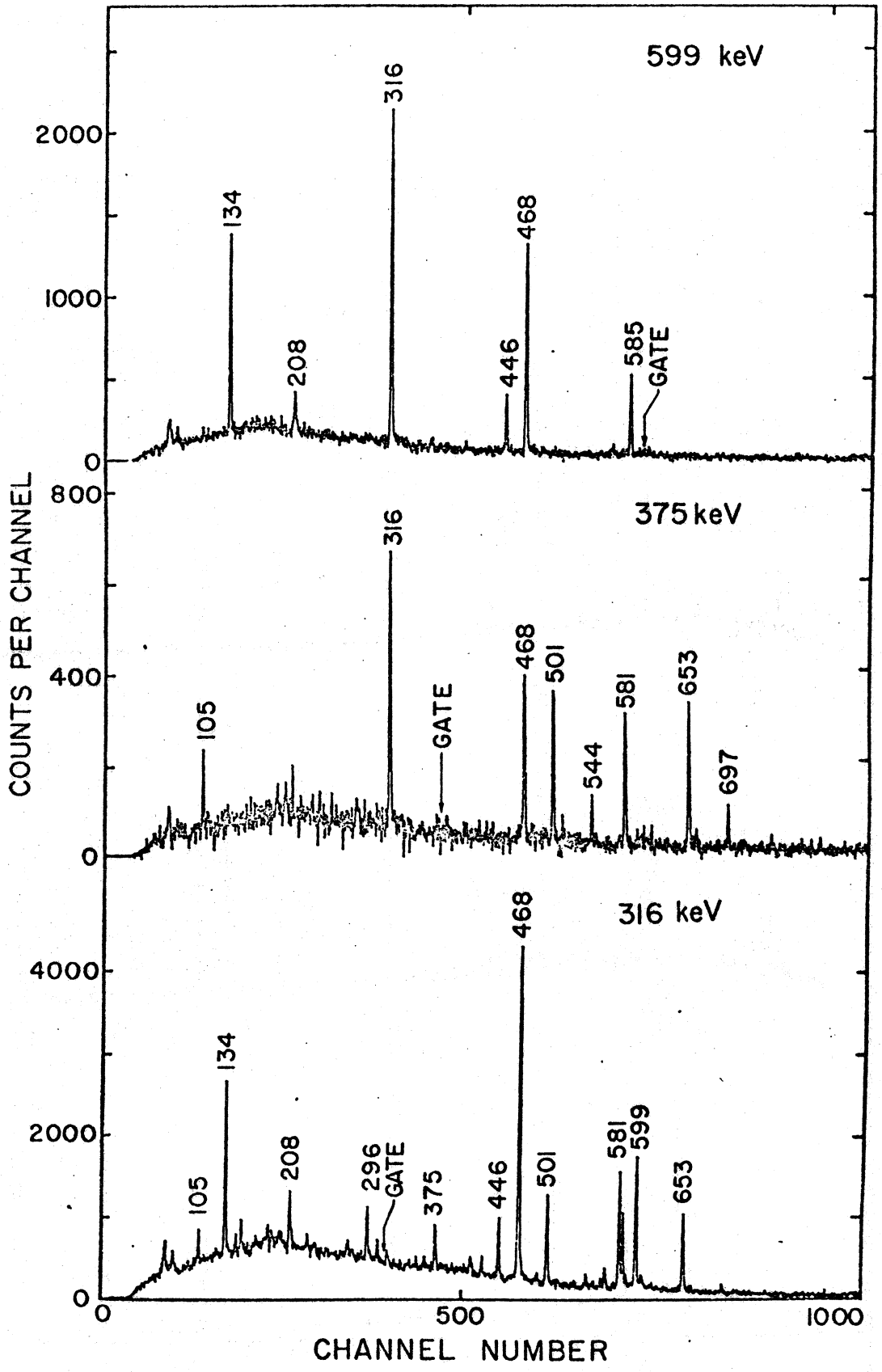
599 keV
316
134
468
208
446
585
GATE
2000
1000
0
375 keV
316
468
501
105
GATE
581
653
544
697
800
400
0
316 keV
468
134
208
296
GATE
375
446
501
581
599
653
105
4000
2000
0
0
500
1000
CHANNEL NUMBER
COUNTS PER CHANNEL

Fig. 2

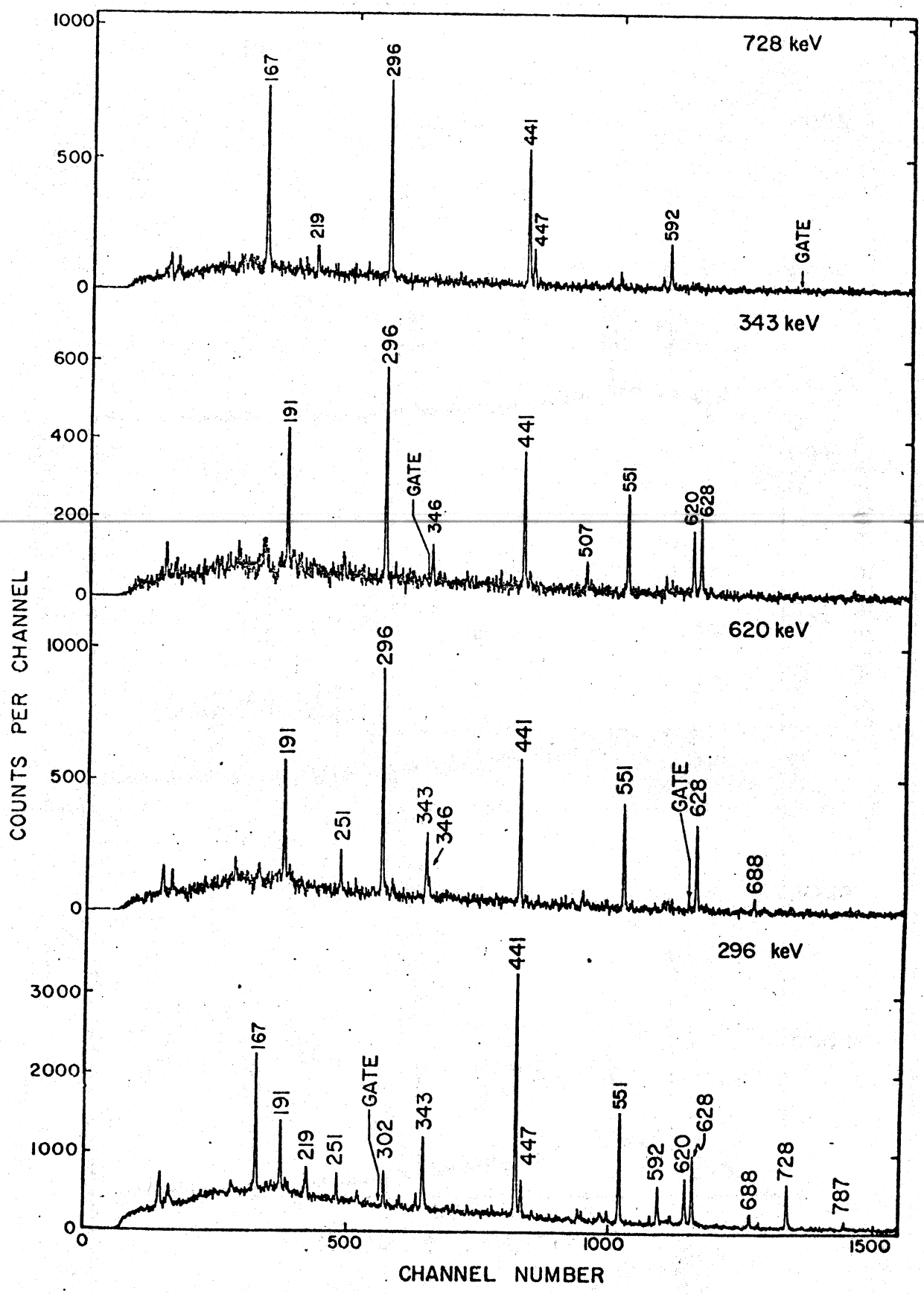
728 keV
167
296
441
219
447
592
GATE
343 keV
296
191
441
GATE
346
551
620
628
507
620 keV
296
191
441
251
343
346
551
GATE
628
688
296 keV
441
167
191
GATE
219
251
302
343
447
551
592
620
628
688
728
787
COUNTS PER CHANNEL
CHANNEL NUMBER
0
500
1000
1500

Fig. 3

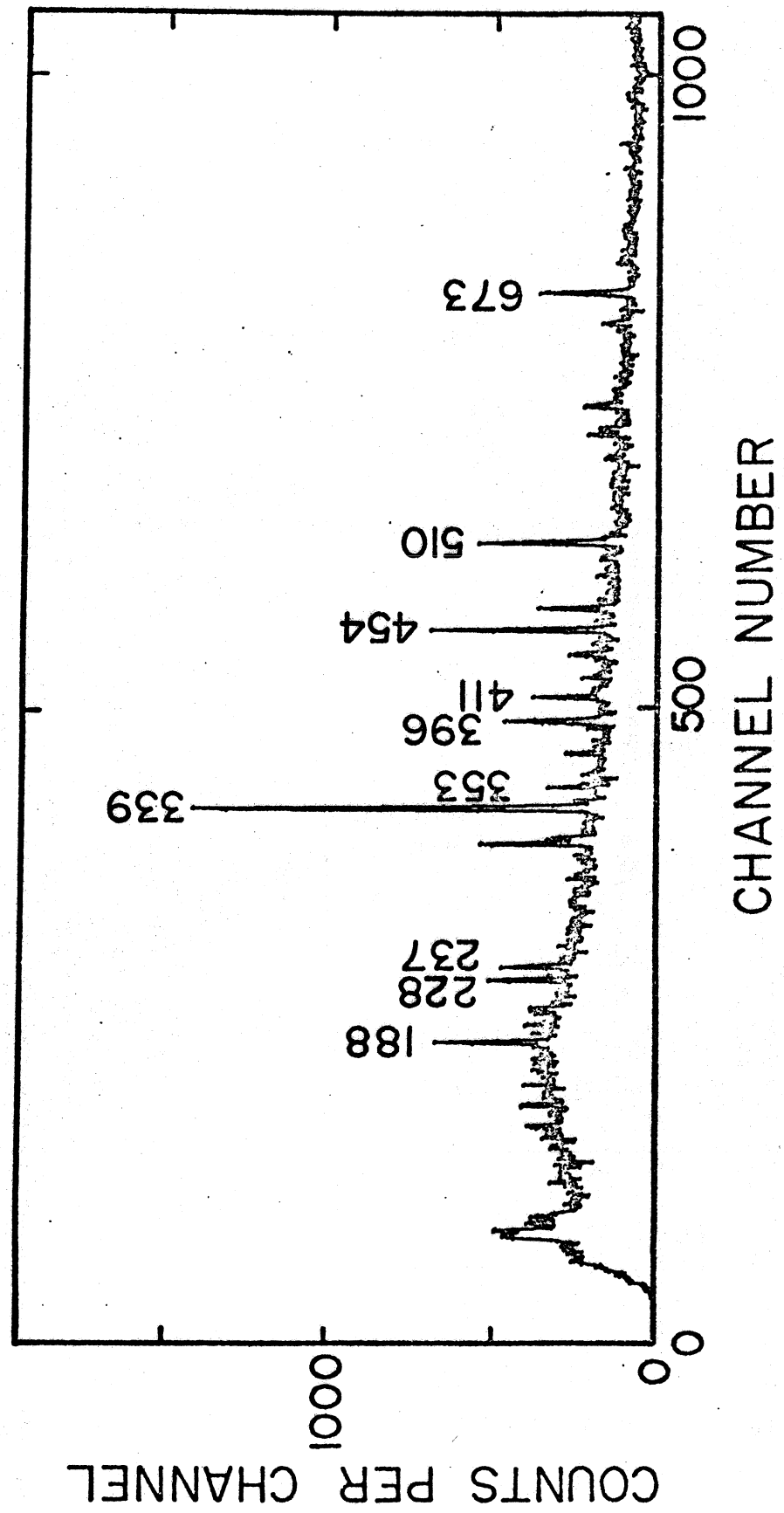
COUNTS PER CHANNEL
1000
0
0
500
1000
CHANNEL NUMBER
673
510
454
411
396
353
339
237
228
188

Fig. 4

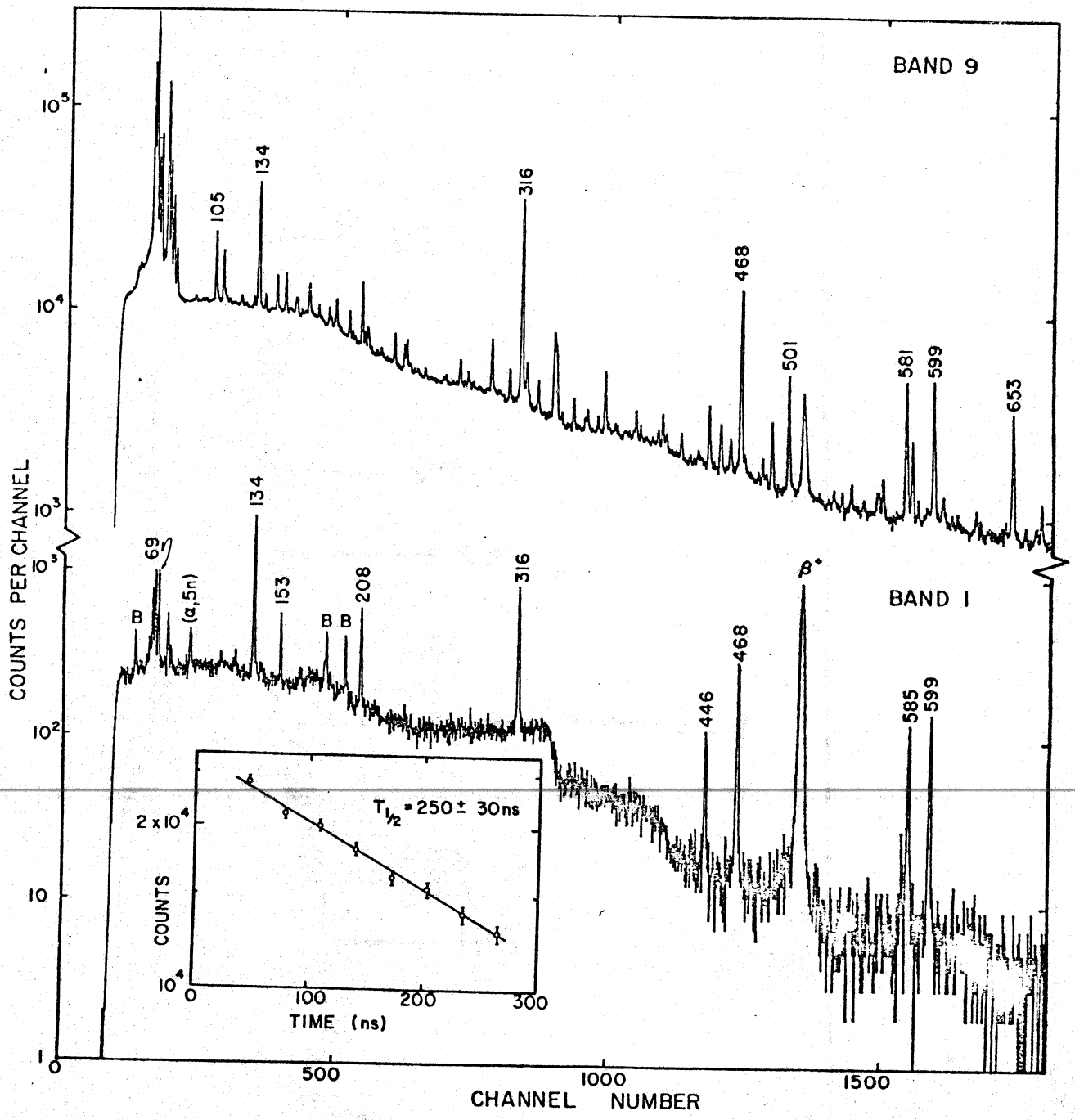
BAND 9
105
134
316
468
501
581
599
653
BAND 1
69
B
(α,5n)
134
153
B B
208
316
β+
446
468
585
599
$T_{1/2}$ = 250 ± 30ns
2 x 10⁴
COUNTS
10⁴
0
100
200
300
TIME (ns)
COUNTS PER CHANNEL
10⁵
10⁴
10³
10³
10²
10
1
0
500
1000
1500
CHANNEL NUMBER

Fig. 5

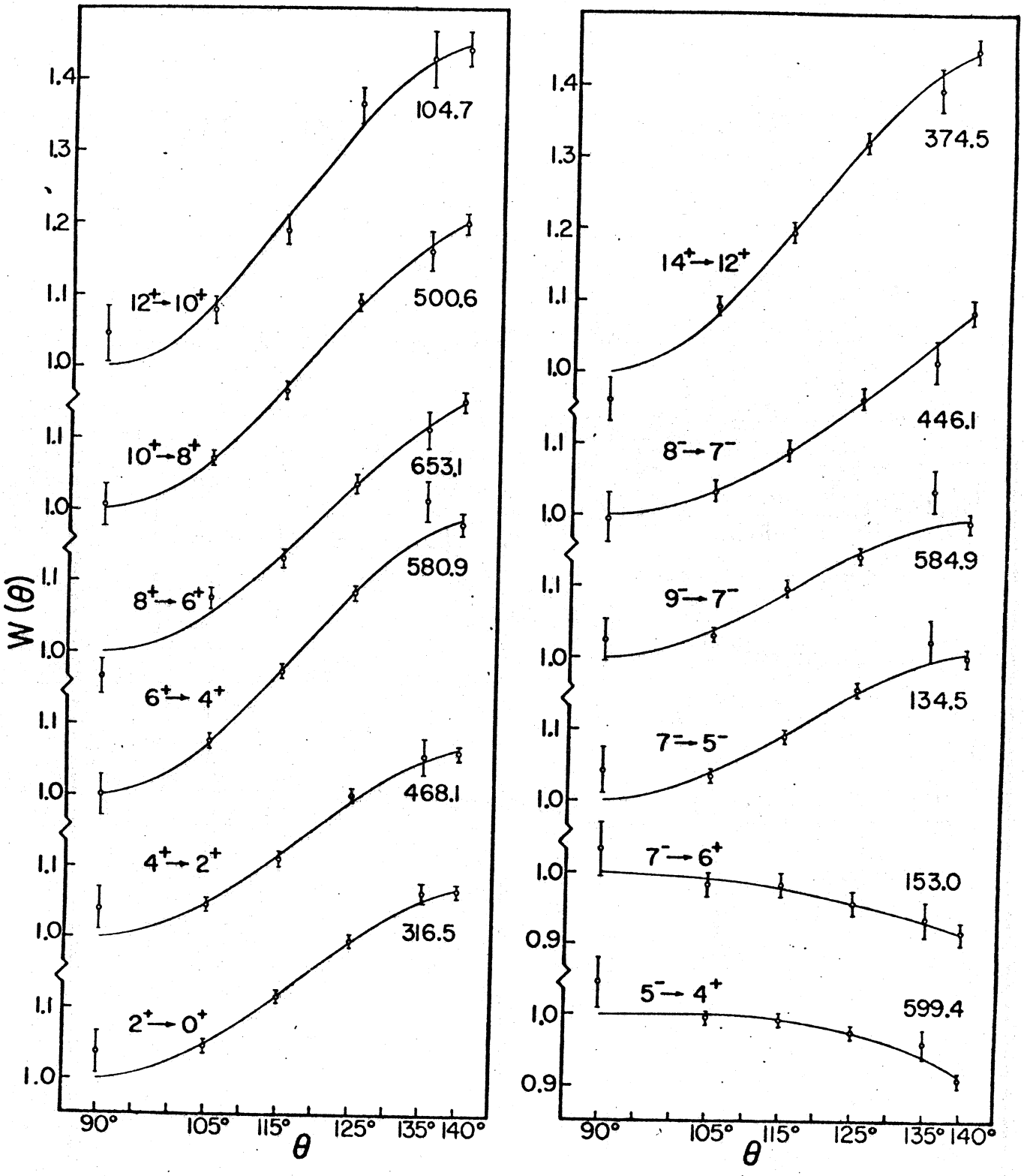
W (θ)
θ
90°
105°
115°
125°
135°
140°
104.7
12⁺→10⁺
500.6
10⁺→8⁺
653.1
8⁺→6⁺
580.9
6⁺→4⁺
468.1
4⁺→2⁺
316.5
2⁺→0⁺
374.5
14⁺→12⁺
446.1
8⁻→7⁻
584.9
9⁻→7⁻
134.5
7⁻→5⁻
153.0
7⁻→6⁺
599.4
5⁻→4⁺

Fig. 6

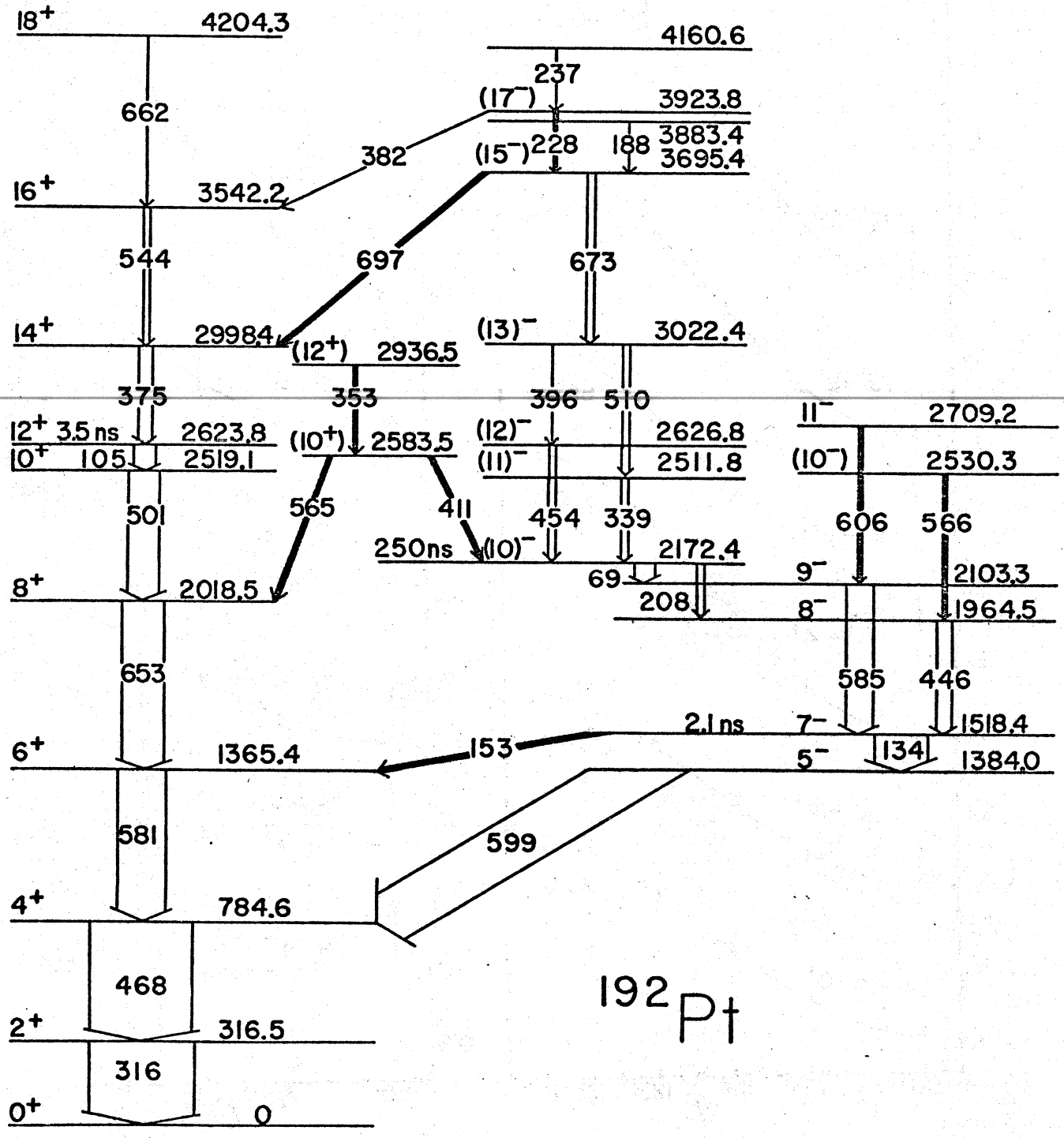
18+ 4204.3
662
16+ 3542.2
544
14+ 2998.4
375
12+ 3.5 ns 2623.8
10+ 105 2519.1
501
8+ 2018.5
653
6+ 1365.4
581
4+ 784.6
468
2+ 316.5
316
0+ 0
4160.6
237
(17−) 3923.8
382
(15−) 228 188 3883.4 3695.4
697
673
(12+) 2936.5
353
(10+) 2583.5
565
411
(13)− 3022.4
396 510
(12)− 2626.8
(11)− 2511.8
454 339
250ns (10)− 2172.4
69
208
11− 2709.2
(10−) 2530.3
606 566
9− 2103.3
8− 1964.5
585 446
2.1ns 7− 1518.4
153
5− 134 1384.0
599
192Pt

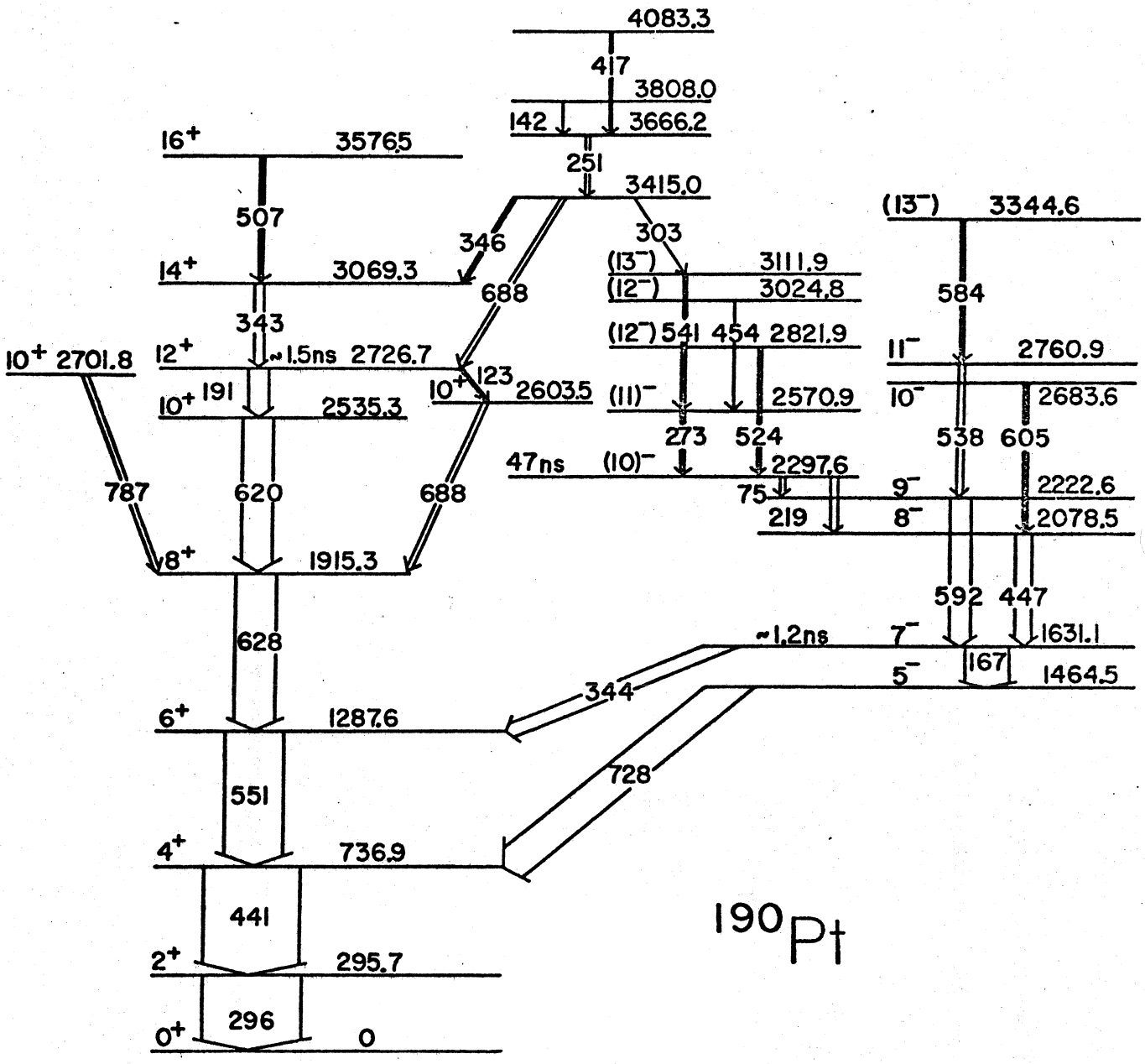
4083.3
417
3808.0
142
3666.2
251
3415.0
303
346
688
16+ 3576.5
507
14+ 3069.3
343
12+ ~1.5ns 2726.7
10+ 2701.8
10+ 191 2535.3
10+ 123 2603.5
787
620
688
8+ 1915.3
628
6+ 1287.6
551
4+ 736.9
441
2+ 295.7
296
0+ 0
(13-) 3111.9
(12-) 3024.8
(12-) 541 454 2821.9
(11)- 2570.9
273 524
47ns (10)- 2297.6
75
219
(13-) 3344.6
584
11- 2760.9
10- 2683.6
538 605
9- 2222.6
8- 2078.5
592 447
~1.2ns 7- 1631.1
167
5- 1464.5
344
728
190Pt